HHS Public Access

Author manuscript

J Biomech. Author manuscript; available in PMC 2022 May 07.

Published in final edited form as:

J Biomech. 2021 May 07; 120: 110348. doi:10.1016/j.jbiomech.2021.110348.

Neuromuscular Compensation Strategies Adopted at the Shoulder Following Bilateral Subpectoral Implant Breast Reconstruction

Joshua M. Leonardis[a], **Whitney L. Wolff**[a], **Adeyiza O. Momoh**[b], **David B. Lipps**[a,c]

[a]School of Kinesiology, University of Michigan, Ann Arbor, MI, USA

[b]Section of Plastic Surgery, University of Michigan, Ann Arbor, MI, USA

[c]Department of Biomedical Engineering, University of Michigan, Ann Arbor, MI, USA

Abstract

Immediate two-stage subpectoral implant breast reconstruction after mastectomy requires the surgical disinsertion of the sternocostal fiber region of the pectoralis major (PM). The disinsertion of the PM would need increased contributions from intact shoulder musculature to generate shoulder torques. This study aimed to identify neuromuscular compensation strategies adopted by subpectoral implant breast reconstruction patients using novel muscle synergy analyses. Fourteen patients treated bilaterally with subpectoral implant breast reconstruction (>2.5 years post-reconstruction) were compared to ten healthy controls. Surface electromyography was obtained from sixteen shoulder muscles as participants generated eight three-dimensional (3D) shoulder torques in five two-dimensional arm postures bilaterally. Non-negative matrix factorization revealed the muscle synergies utilized by each experimental group on the dominant and non-dominant limbs, and the normalized similarity index assessed group differences in overall synergy structure. Bilateral subpectoral implant patients exhibited similar shoulder strength to healthy controls on the dominant and non-dominant arms. Our results suggest that 3D shoulder torque is driven by three shoulder muscle synergies in both healthy participants and subpectoral implant patients. Two out of three synergies were more similar than is expected by chance between the groups on the non-dominant arm, whereas only one synergy is more similar than is expected by chance on the dominant arm. While bilateral shoulder strength is maintained following bilateral subpectoral implant breast reconstruction, a closer analysis of the muscle synergy patterns underlying 3D shoulder torque generation reveals that subpectoral implant patients adopt compensatory neuromuscular strategies only with the dominant arm.

Corresponding Author: David B. Lipps, PhD, 401 Washtenaw Ave., CCRB 3730, Ann Arbor, MI 48109, Tel. +1 734-647-3131, Fax. +1 734-936-1925, dlipps@umich.edu.

CONFLICT OF INTEREST STATEMENT

The authors do not have any financial or personal relationships to disclose that could have inappropriately biased this work.

Keywords

Breast cancer; breast reconstruction; muscle synergy; neuromuscular system; electromyography

1. INTRODUCTION

Women with primary breast cancer are increasingly being managed with a mastectomy to excise all breast tissue (Albornoz et al., 2015; Habermann et al., 2010). The rising mastectomy rate is partly driven by more women diagnosed with unilateral disease opting to undergo bilateral mastectomies for prophylactic reasons (Cemal et al., 2013; Jagsi et al., 2017; Metcalfe et al., 2008; Yao et al., 2010) combined with improved availability of post-mastectomy breast reconstruction options to restore the breast mound (Al-Ghazal et al., 2000; Alderman et al., 2003; Chang et al., 2016; Habermann et al., 2014; McGuire et al., 2009). Immediate two-stage subpectoral implant breast reconstruction accounts for 69% of all post-mastectomy breast reconstructions (Surgeons, 2019). This approach occurs during the same procedures as mastectomy and requires the surgical division of the sternocostal fiber region of the pectoralis major (PM) from the inferior pole of the breast to the sternum to place a tissue expander and eventual implant beneath the muscle.

The PM is critical for the generation of shoulder flexion, adduction, and internal rotation torques, and the maintenance of shoulder stiffness (Ackland et al., 2008; Halder et al., 2001; Jansen et al., 2005; Kuechle et al., 1997; Leonardis et al., 2019; Stegink-Jansen et al., 2011). Additionally, the PM is also a primary contributor to motion of the scapula. Altered PM length may result in altered scapular motion (Borstad and Ludewig, 2005). Clinicians assume the remaining, intact shoulder muscles increase their contributions to shoulder function following the disinsertion of the PM (Spear and Hess, 2005). The remaining intact regions of the PM reorganize their contributions to shoulder function after subpectoral implant breast reconstruction (Hage et al., 2014; Leonardis et al., 2019). However, it remains unknown whether the entire shoulder musculature compensates for the division of the PM during breast reconstruction.

The shoulder complex is an indeterminate system, where identical shoulder torques can be generated by altering the timing and magnitude of synergistic muscles. The central nervous system simplifies the solution space for such a problem by using a single neural command to activate low-dimensional groups of muscles, henceforth referred to as muscle synergies (Bizzi et al., 2008; Flash and Hochner, 2005; Tresch et al., 2002). Muscle synergies are commonly derived using the decomposition of experimental sEMG data into a set of synergy vectors that describe the weighted contributions of a given number of muscles to a set of experimental tasks. Overall muscle synergy structure remains robust across healthy participants performing unilateral reaching tasks but is influenced by arm dominance (Coscia et al., 2014; de Freitas et al., 2007; Duthilleul et al., 2015; Krishnamoorthy et al., 2003; Roh et al., 2012). Synergy structure is also influenced by neurological pathology (Cheung et al., 2012; Roh et al., 2013; Steele et al., 2015). Neuromuscular pathologies reduce neuromuscular complexity, resulting in fewer synergies required to adequately describe experimental sEMG data (Clark et al., 2010; Steele et al., 2015). As patients increasingly elect for bilateral mastectomy and breast reconstructions, it is unknown if arm dominance and/or disinsertion of the PM influence neuromuscular adaptations to surgery.

Therefore, the purpose of this study was to identify the neuromuscular compensation strategies adopted by patients previously treated with mastectomy and subpectoral implant breast reconstruction. We hypothesized that subpectoral implant breast reconstruction patients (when compared to healthy controls) would exhibit decreased pectoralis major and increased latissimus dorsi and teres major surface EMG amplitudes, different structure of shoulder muscle synergies, and reduced neuromuscular complexity (as evidenced by fewer synergies and greater variance accounted for by the first synergy) on both the dominant and non-dominant arms.

2. METHODS

2.1 Participants

Twenty-four women participated in a single experimental session. Fourteen women previously received a mastectomy and subpectoral implant breast reconstruction from the same surgeon (A.O.M) at the University of Michigan between 2014 and 2017. Inclusion criteria required patients to have had mastectomy and breast reconstruction during the same surgical visit, the reconstruction must have disinserted the sternocostal fiber region of the PM from the inferior and medial pole of the breast onto the sternum, and patients must have been a minimum of 18 months post-reconstruction. Ten healthy, age-matched participants were recruited from the Ann Arbor and University of Michigan communities. Participants with a history of upper extremity neuromuscular or orthopaedic conditions, radiotherapy, current shoulder pain or pathology, or breast augmentation surgery were excluded. Participants provided informed consent before the collection of any data. Study procedures were approved by the University of Michigan’s Institutional Review Board (HUM00114801/HUM00111519).

2.2 Experimental Procedures

Experimental procedures were completed in a single session. Both arms were examined with the order randomized. Activation data were obtained from 16 shoulder muscles using single differentiated, pre-amplified sEMG electrodes (DE – 2.1 sensors; gain 1000x, Bagnoli system, Delsys, Natick, MA). A detailed description of our preparation and electrode placement procedures are previously published (Leonardis et al., 2020).

Maximal voluntary contractions (MVC) were obtained at the onset of experimental procedures in a single shoulder posture (15° plane of elevation and 75° elevation) on both arms. This posture was chosen to represent a place in the center of the workspace of the upper extremity and was used to avoid inducing fatigue from repeated maximal contractions in multiple postures. Participants generated maximal isometric shoulder torques in the positive and negative direction of each plane of measurement (plane of elevation (Θ); elevation (Φ); rotation (Ψ)). Verbal motivation and adequate rest between maximal exertions were provided.

Participants were examined bilaterally in five postures: 15° plane of elevation combined with 75° elevation and every combination of two plane of elevation (0°, 45°) and elevation (45°, 105°) angles (Figure 1A, B). These postures were chosen to represent the center and outer edges of the upper extremity workspace utilized in the current study. The order of postures was randomized within each arm. In each posture, participants generated and maintained three-dimensional (3D) shoulder torques for two seconds in every combination of plane of elevation (±Θ), elevation (±Φ), and rotation (±Ψ) (Figure 1C). Each torque component was scaled to 20% of the participant's lowest recorded MVC to ensure satisfactory execution and avoid fatigue. The order in which torques were presented within each posture was randomized. Visual feedback was provided to assist participants with torque accuracy. Adequate rest was provided between trials. In total, participants performed 80 individual trials (8 torques × 5 postures × 2 arms).

2.3 Data Analyses

Surface electromyography data were analyzed in MATLAB 2017a (Mathworks Inc, Natick, MA). Data were band-pass filtered between 20 and 450 Hz, rectified, detrended, low-pass filtered at 6 Hz, averaged with a 200ms moving window, and normalized to the muscle's maximum obtained across all MVCs and experimental trials. Synergies were derived using non-negative matrix factorization (NNMF) in MATLAB (nnmf, alternating least squares). NNMF decomposes a matrix of experimental data (A) into synergy (W) and coefficient (C) matrices by minimizing the root-mean-squared error between experimental (A) and reconstructed data ($W \cdot C$). The dimensions of synergy matrices represent the number of included muscles (16) and a user-defined number of synergies (N_W). Our analysis was iterated with N_W beginning at one and increasing by one until reconstructed data accounted for greater than 95% of the variance in experimental data. To avoid local minima, we repeated this analysis 10 times for each participant and arm, yielding 480 unique sets of synergies (24 participants × 2 arms × 10 repetitions).

The comparison of synergies across arms and experimental groups required a previously described organization algorithm (Leonardis et al., 2020). This algorithm utilizes the normalized similarity index (SI), which is reported on a scale from 0–1, where 1 means two synergies are identical. The minimum SI to determine if two synergies were more similar than is expected by chance was set at 0.63, which corresponds to the critical value of Pearson's r at $p=0.01$ for 14 degrees of freedom (16 muscles – 2) (Chvatal and Ting, 2013). Neuromuscular complexity was quantified using N_{95} and $tVAF_1$, where N_{95} represents the number of synergies required to account for more than 95% of the variance in experimental data, and $tVAF_1$ represents the variance accounted for b the first, principal synergy. A larger N_{95} and smaller $tVAF_1$ are indicative of greater complexity (Schwartz et al., 2016; Steele et al., 2015).

2.4 Statistical Analysis

We performed an *a priori* sample size calculation using muscle activity data from three shoulder muscles previously reported in mastectomy patients (Shamley et al., 2007). This power analysis revealed that a minimum sample size of 20 participants (10 per group) was required to detect significant between-group differences in sEMG amplitudes using a linear mixed effects model with alpha = 0.05 and 80% power. We attempted to recruit 28 total participants (14 per group) to fully ensure power. While we entirely recruited the reconstruction cohort, the healthy control group was limited to 10 participants due to the onset of the COVID-19 pandemic.

All statistical tests were performed in SPSS (v24, IBM Corporation, Chicago, IL, USA). Independent t-tests examined group differences in demographic variables. Shoulder strength was assessed using separate linear mixed effects models for each strength measure (*flexion, extension, adduction, abduction, internal rotation, external rotation*) where arm dominance (*dominant, non-dominant*) and experimental group (*subpectoral implant, control*) were fixed factors and random intercepts controlled for variability at the subject level. To assess group differences in EMG amplitudes, we utilized a separate linear mixed effects model for each shoulder muscle. In these models, arm dominance and experimental group were fixed factors, sEMG amplitude was the outcome measure, and random intercepts controlled for subject-specific. Bonferroni corrections were performed when applicable and all relevant interactions were assessed.

To test our hypothesis that the structure of shoulder muscle synergies derived from subpectoral implant breast reconstruction patients would differ from those derived from healthy participants we computed the SI between each synergy derived from each subpectoral implant participant and that synergy's analog derived from the same side (*dominant, non-dominant*) in every healthy control participant. Descriptive statistics were then used to explore the influence of experimental group and arm dominance on muscle synergy composition. We assessed group differences in neuromuscular complexity using a Kruskal-Wallis test to examine the influence of group and arm dominance on the number of synergies required to account for more than 95% of the variance in experimental data (N_{95}). Rank sum post hoc tests were used when applicable. A linear mixed effects model examined the influence of arm dominance and experimental group on the total variance accounted for by the first, principal synergy ($tVAF_1$).

3. RESULTS

3.1 Patient Demographics and Strength

No group differences existed in age ($t_{22}=1.61$, $p=0.12$), height ($t_{22}=-1.88$, $p=0.09$), or BMI ($t_{22}=-1.56$, $p=0.09$). However, subpectoral implant participants were heavier than controls ($t_{22}=-2.11$, $p=0.03$). Subpectoral implant participants were an average (SEM) of 1,019 (83) days post-reconstruction. The minimum time post-reconstruction was 581 days while the maximum was 1523. Additional participant information is provided in Table 1. There was no significant effect of the group (all $F_{1,19}\leq 1.031$, $p=0.323$) or arm dominance (all $F_{1,17}\leq 0.837$, $p=0.373$) on any shoulder strength measure. Additionally, no group × arm dominance interactions were observed for any strength measure (all $F_{1,17}\leq 2.86$, $p=0.110$) (Figure 2).

3.2 Shoulder Muscle Activity

Surface EMG recorded activity from 16 upper extremity muscles while participants generated eight 3D shoulder torques in five arm postures bilaterally. We found no main effect of group on sEMG amplitude for any shoulder muscle (all $F_{1,23} \leq 3.70, p \geq 0.067$). We observed a main effect of arm dominance on sEMG amplitude for the sternocostal fiber region of the pectoralis major, middle deltoid, upper trapezius, lower trapezius, latissimus dorsi, teres major, infraspinatus, biceps brachii long head, brachioradialis, and triceps brachii lateral head (all $F_{1,1537} \geq 6.81$, $p \leq 0.009$). sEMG amplitude was greater on the non-dominant arm for the upper trapezius, teres major, and biceps brachii (all $p<0.001$), while the remaining muscles exhibited greater activity on the dominant arm (all $p \leq 0.009$). A group × arm dominance interaction was observed only in the sternocostal fiber region of the pectoralis major and the upper trapezius (both $F_{1,1537} \geq 89.1, p<0.001$) (Figure 3). Post-hoc comparisons found that the sternocostal fiber region exhibited greater sEMG amplitude for the non-dominant arm in healthy controls when compared to subpectoral implant participants ($p=0.017$). The upper trapezius exhibited greater activity in control participants on the dominant arm ($p=0.002$), and greater activity in subpectoral implant patients on the non-dominant arm ($p=0.027$).

3.3 Shoulder Muscle Synergies

Muscle synergies analyses described the coordinated activity of shoulder muscles extremely well. Across participants, the derived synergies accounted for 96% (0.7) (mean (SEM)) of the variance in experimental data. The number of synergies varied from 1 to 3 and depended on participant and arm. In general, the derived synergies fell into one of three distinct groups. The first synergy group was characterized largely by the fiber regions of the pectoralis major and the brachioradialis. The second group was characterized by the middle deltoid, lower trapezius, and lateral head of the triceps brachii. The third was made up of varying contributions from the middle and lower trapezius, long head of the biceps brachii, and the brachioradialis. Synergies derived from representative participants from each experimental group can be found in Figure 4. When averaged across all participants, the overall structure of synergies remained extremely similar, with only slight variations in the weighting of individual muscles (Figure 5). Thirty-eight percent of all derived synergies fell into the first group (Synergy 1), 32% fell into the second (Synergy 2), and 30% fell into the third (Synergy 3). All three Synergies were represented equally on the dominant (first/second/third synergy: 34/31/35%) and non-dominant (37/33/30%) limbs of controls as well as on the non-dominant arm (40/30/30%) of subpectoral implant patients. However, Synergy 3 accounted for only 21% of all derived synergies on the dominant arm of subpectoral implant patients.

To assess the influence of experimental group and arm dominance on the overall structure of our derived synergies, we computed the SI between the synergies derived from every subpectoral implant participant and their analogs derived from the same side in every healthy control participant. This resulted in a total of 429 similarity indices. Of these, 62% fell above the 0.63 threshold that corresponds to the critical value of Pearson's r at $p=0.01$. When investigating the influence of arm dominance on the synergy structure, we found that only Synergy 2 was more similar than is expected by chance between the groups (mean

(SEM) SI: 0.71 (0.02)) on the dominant arm (Figure 6). A mean (SEM) SI of 0.62 (0.2) and 0.62 (0.03) was computed for Synergies 1 and 3, respectively. On the non-dominant arm, Synergies 1 and 2 were more similar than is expected by chance between groups. Synergy 3 derived from the non-dominant arm was not similar between the groups (mean (SEM) SI: 0.57 (0.02)).

3.4 Neuromuscular Complexity

The number of muscle synergies needed to account for 95% of variance in experimental data (N_{95}), and the variance accounted for by the first, principal synergy (VAF_1) are two measures of neuromuscular complexity. We utilized these metrics to examine the neuromuscular impairment associated with subpectoral implant breast reconstruction. We found that N_{95} did not differ by group ($\chi^2_{(1,39)}=1.69, p=0.192$), arm dominance ($\chi^2_{(1,39)}=0.581, p=0.446$), or by group within each arm (both $\chi^2_{(1,189)}\leq 2.48, p\geq 0.115$). Similarly, we found no effect of group ($F_{1,18}= 0.381, p=0.544$) or arm dominance ($F_{1,18}= 0.108, p=0.746$) on VAF_1. No interaction between group and arm dominance on VAF_1 was observed ($F_{1,18}= 0.180, p=0.677$).

4. DISCUSSION

The current study provides the first examination of neuromuscular compensation strategies adopted by breast cancer patients treated bilaterally with mastectomy and subpectoral implant breast reconstruction. We hypothesized that subpectoral implant breast reconstruction patients (when compared to healthy controls) would exhibit decreased pectoralis major and increased latissimus dorsi and teres major surface EMG amplitudes. This hypothesis was not accepted as both groups exhibited similar surface EMG amplitudes. We also hypothesize that our experimental groups would exhibit different shoulder muscle synergy structure, regardless of arm dominance. This hypothesis was partially accepted, as synergies were far less similar between subpectoral implant patients and age-matched controls only for the dominant arm. Finally, we hypothesized that subpectoral implant patients would exhibit reduced neuromuscular complexity (as evidenced by fewer synergies and greater variance accounted for by the first synergy) on both the dominant and non-dominant arms. However, neuromuscular complexity was unaltered by subpectoral implant breast reconstruction, regardless of arm. Together, these findings suggest that patients treated bilaterally with mastectomy and subpectoral implant breast reconstruction maintain shoulder function and neuromuscular complexity by altering neuromuscular control of the dominant arm more so than the non-dominant arm.

The successful execution of activities of daily living requires adequate bilateral shoulder strength. Subpectoral implant breast reconstruction requires the surgical disinsertion of the sternocostal fiber region of the PM, which is expected to influence shoulder strength. As such, previous investigations revealed significant reductions in shoulder strength for subpectoral implant breast reconstruction patients more than 1-year post-reconstruction (de Haan et al., 2007; Leonardis et al., 2019). However, these findings did not account for arm dominance. We observed comparable shoulder strength for the dominant and non-dominant arms of bilateral subpectoral implant patients that were, on average, 2.5 years post-reconstruction when compared to healthy control participants. None of the bilateral subpectoral implant patients included in the current study underwent any post-surgical rehabilitation. Therefore, findings from the current study suggest that mastectomy and subpectoral implant breast reconstruction may not reduce shoulder strength, or given enough time for recovery, that shoulder strength is maintained. Our findings may also differ with prior literature due to differences in the posture used to obtain strength measurements and an increased time to recover from surgery.

Clinicians often assume that the neuromusculoskeletal system compensates for lost function due to muscle disinsertion by recruiting synergist muscles (Olivari, 1976; Quillen, 1979; Spear and Hess, 2005). The similarity in shoulder strength observed between our experimental groups suggests that bilateral subpectoral implant patients must adopt neuromuscular compensation strategies to maintain shoulder function. Surface EMG data pooled across dominant and non-dominant arms suggest that healthy control participants and bilateral subpectoral implant patients activate shoulder musculature similarly. On the dominant arm, only upper trapezius activity differed between our groups, with the subpectoral implant patients reducing its activity. On the non-dominant arm, bilateral subpectoral implant patients exhibited reduced sternocostal fiber region activity and increased upper trapezius activity. However, a comparison of surface EMG amplitudes provides little information regarding the synchronous activity of numerous shoulder musculature.

We employed muscle synergy analyses to explore the influence of bilateral subpectoral implant breast reconstruction on the coordinated contributions of shoulder musculature. The structure of these synergies differed between the dominant and non-dominant arms of subpectoral implant patients when compared to age-matched controls. We found that only Synergies 1 and 2 were more similar than is to be expected by chance between the groups on the non-dominant arm. On the dominant arm, however, only Synergy 2 was more similar than is expected by chance between the groups. Synergy 1 is characterized by primary contributions from the fiber regions of the PM. A reduction in contributions from the sternocostal fiber region of the PM, which is compromised during subpectoral implant breast reconstruction, is likely driving differences in the structure of Synergy 1 between the groups on the dominant arm. It must also be noted that there are large variances in SI regardless of synergy or arm. We believe this is largely a function of the inherent complexity of neuromuscular control, especially during the execution of complex shoulder torques. Variance was particularly large in the SI generated for Synergy 1 on the dominant arm. This may be due to the variation in the volume of pectoralis major disinserted during subpectoral implant breast reconstruction. We took steps to control for this variation by recruiting participants from a single surgeon’s practice, but individual participant anatomy plays a larger role in the volume of pectoralis major disinserted than does the surgeon performing the procedure. This is an interesting area of future research.

The current study is the first to provide empirical evidence that the neuromuscular system is capable of compensating for the removal of the inferior attachments of the PM. This was determined by assessing the changes in neuromuscular complexity at the shoulder. Neuromuscular complexity is reduced following neurological events such as stroke and cerebral palsy (Cheung et al., 2012; Roh et al., 2013; Steele et al., 2015), where the resultant muscle weakness reduces the degrees of freedom available. The current study is the first to consider a clinical situation where an otherwise intact nervous system must maintain control of an intact joint after irreparable damage to key shoulder musculature (e.g., the disinsertion of the PM). It is reasonable to believe that compromising the function of a key shoulder muscle would influence neuromuscular control of the shoulder joint by reducing the degrees of freedom available to the nervous system. However, we found bilateral subpectoral implant patients exhibited similar complexity to healthy controls, regardless of arm dominance. Combined with our findings regarding synergy structure, this suggests that bilateral subpectoral implant patients maintain neuromuscular complexity by altering overall muscle synergy structure on their dominant arm and maintaining synergy structure on their non-dominant. Together, these findings confirm the neuromuscular system compensates for the disinsertion of the PM.

The current study possessed several limitations. First, muscle fatigue may influence surface EMG data. We selected submaximal torques for the current study that are far below the feasible torques for the shoulder and should not produce fatigue (Baillargeon et al., 2019). Additionally, participants were provided as much time as needed between trials within each posture, and several minutes of rest were given between postures. We also randomized the order or postures and trials within each posture so as to reduce the effects of fatigue on our results. Shoulder muscle sEMG amplitudes are also influenced by changes in posture (Antony and Keir, 2010; Kronberg et al., 1990; Wickham et al., 2010). We only obtained surface EMG data was only collected from 16 shoulder muscles, as some rotator cuff muscles were omitted because they require intramuscular EMG to obtain accurate data (Xu et al., 2014). The muscles included here represent primary movers of the shoulder and scapula, although the accuracy of sEMG data obtained from the serratus has been disputed (Hackett et al., 2014). The inclusion of additional shoulder musculature would improve the identification of shoulder muscle synergies (Antony and Keir, 2010; Kronberg et al., 1990; Steele et al., 2013; Wickham et al., 2010). The shoulder possesses the largest range of motion of any joint in the human body. However, we only assessed five postures to reduce fatigue. These postures represent the full workspace in which the majority of activities of daily living occur. Shoulder muscle sEMG amplitudes are changed with posture (Antony and Keir, 2010; Kronberg et al., 1990; Wickham et al., 2010). The arm postures did not include changing the rotation angle or elbow flexion angle. Our findings are limited to the examined postures and cannot extend to postures with differing humeral rotation, elbow flexion, or scapular motion. Assessing a larger number of arm postures would provide greater insight into the effects of mastectomy and subpectoral implant breast reconstruction on neuromuscular control of the shoulder.

5. CONCLUSIONS

In conclusion, the current study revealed 3D shoulder torque generation is driven by three shoulder muscle synergies in both healthy and subpectoral implant patients. However, the structure of these synergies was only more similar than is expected by chance between healthy and subpectoral implant patients for the non-dominant arm. Bilateral subpectoral implant patients exhibited similar complexity to healthy controls, regardless of arm dominance. This suggests that bilateral subpectoral implant patients maintain neuromuscular complexity by altering overall muscle synergy structure on their dominant arm and maintaining their synergy structure on their non-dominant. These results provide the first evidence of subpectoral implant patients adopting neuromuscular compensation strategies at the shoulder.

ACKNOWLEDGMENTS

This research was supported by the Eunice Kennedy Shriver National Institute for Child Health and Human Development of the National Institutes of Health under award number R03HD097704, along with the University of Michigan's Rackham Graduate School Predoctoral Fellowship Program. The study sponsors had involvement in the collection, analysis, data interpretation, or writing of this manuscript.

REFERENCES

Ackland DC, Pak P, Richardson M, Pandy MG, 2008. Moment arms of the muscles crossing the anatomical shoulder. J. Anat 213, 383–390. [PubMed: 18691376]

Al-Ghazal S, Fallowfield L, Blamey R, 2000. Comparison of psychological aspects and patient satisfaction following breast conserving surgery, simple mastectomy and breast reconstruction. Eur. J. Cancer 36, 1938–1943. [PubMed: 11000574]

Albornoz CR, Matros E, Lee CN, Hudis CA, Pusic AL, Elkin E, Bach PB, Cordeiro PG, Morrow M, 2015. Bilateral mastectomy versus breast-conserving surgery for early stage breast cancer: the role of breast reconstruction. Plast. Reconstr. Surg 135, 1518. [PubMed: 26017588]

Alderman AK, McMahon L, Wilkins EG, 2003. The national utilization of immediate and early delayed breast reconstruction and the effect of sociodemographic factors. Plast. Reconstr. Surg 111, 695–705. [PubMed: 12560690]

Antony NT, Keir PJ, 2010. Effects of posture, movement and hand load on shoulder muscle activity. J. Electromyogr. Kinesiol 20, 191–198. [PubMed: 19473855]

Baillargeon EM, Ludvig D, Sohn MH, Nicolozakes CP, Seitz AL, Perreault EJ, 2019. Experimentally quantifying the feasible torque space of the human shoulder. J. Electromyogr. Kinesiol

Bizzi E, Cheung V, d'Avella A, Saltiel P, Tresch M, 2008. Combining modules for movement. Brain Res. Rev 57, 125–133. [PubMed: 18029291]

Borstad JD, Ludewig PM, 2005. The effect of long versus short pectoralis minor resting length on scapular kinematics in healthy individuals. J. Orthop. Sports Phys. Ther 35, 227–238. [PubMed: 15901124]

Cemal Y, Albornoz CR, Disa JJ, McCarthy CM, Mehrara BJ, Pusic AL, Cordeiro PG, Matros E, 2013. A paradigm shift in US breast reconstruction: Part 2. The influence of changing mastectomy patterns on reconstructive rate and method. Plast. Reconstr. Surg 131, 320e–326e.

Chang JM, Kosiorek HE, Dueck AC, Casey WJ, Rebecca AM, Mahabir R, Patel SH, Keole SR, Wong WW, Vargas CE, 2016. Trends in mastectomy and reconstruction for breast cancer; a twelve year experience from a tertiary care center. The American Journal of Surgery 212, 1201–1210. [PubMed: 27866726]

Cheung VC, Turolla A, Agostini M, Silvoni S, Bennis C, Kasi P, Paganoni S, Bonato P, Bizzi E, 2012. Muscle synergy patterns as physiological markers of motor cortical damage. PNAS 109, 14652–14656. [PubMed: 22908288]

Chvatal SA, Ting LH, 2013. Common muscle synergies for balance and walking. Front. Comput. Neurosci 7, 48. [PubMed: 23653605]

Clark DJ, Ting LH, Zajac FE, Neptune RR, Kautz SA, 2010. Merging of healthy motor modules predicts reduced locomotor performance and muscle coordination complexity post-stroke. J. Neurophysiol 103, 844–857. [PubMed: 20007501]

Coscia M, Cheung VC, Tropea P, Koenig A, Monaco V, Bennis C, Micera S, Bonato P, 2014. The effect of arm weight support on upper limb muscle synergies during reaching movements. J. Neuroeng. Rehabil 11, 22. [PubMed: 24594139] de Freitas PB, Krishnan V, Jaric S, 2007. Force coordination in static manipulation tasks: effects of the change in direction and handedness. Exp. Brain Res 183, 487–497. [PubMed: 17665176]

de Haan A, Toor A, Hage JJ, Veeger HE, Woerdeman LA, 2007. Function of the pectoralis major muscle after combined skin-sparing mastectomy and immediate reconstruction by subpectoral implantation of a prosthesis. Ann. Plast. Surg 59, 605–610. [PubMed: 18046138]

Duthilleul N, Pirondini E, Coscia M, Micera S, 2015. Effect of handedness on muscle synergies during upper limb planar movements. 37th Annual International Conference of the IEEE Engineering in Medicine and Biology Society.

Flash T, Hochner B, 2005. Motor primitives in vertebrates and invertebrates. Curr. Opin. Neurobiol 15, 660–666. [PubMed: 16275056]

Habermann EB, Abbott A, Parsons HM, Virnig BA, Al-Refaie WB, Tuttle TM, 2010. Are mastectomy rates really increasing in the United States? J. Clin. Oncol 28, 3437–3441. [PubMed: 20548000]

Habermann EB, Thomsen KM, Hieken TJ, Boughey JC, 2014. Impact of availability of immediate breast reconstruction on bilateral mastectomy rates for breast cancer across the United States: data from the nationwide inpatient sample. Ann. Surg. Oncol 21, 3290–3296. [PubMed: 25052247]

Hackett L, Reed D, Halaki M, Ginn KA, 2014. Assessing the validity of surface electromyography for recording muscle activation patterns from serratus anterior. J. Electromyogr. Kinesiol 24, 221–227. [PubMed: 24534053]

Hage JJ, van der Heeden JF, Lankhorst KM, Romviel SM, Vluttters ME, Woerdeman LA, Visser B, Veeger H, 2014. Impact of combined skin sparing mastectomy and immediate subpectoral prosthetic reconstruction on the pectoralis major muscle function: a preoperative and postoperative comparative study. Ann. Plast. Surg 72, 631–637. [PubMed: 23486118]

Halder A, Zhao KD, O'Driscoll S, Morrey B, An K-N, 2001. Dynamic contributions to superior shoulder stability. J. Orthop. Res 19, 206–212. [PubMed: 11347692]

Jagsi R, Hawley ST, Griffith KA, Janz NK, Kurian AW, Ward KC, Hamilton AS, Morrow M, Katz SJ, 2017. Contralateral prophylactic mastectomy decisions in a population-based sample of patients with early-stage breast cancer. JAMA Surg 152, 274–282. [PubMed: 28002555]

Jansen C, Buford W, Patterson T, Gould L, 2005. A model of length increases of the pectoralis major muscle to provide rehabilitation precautions for patients after mastectomy, 27th Annual International Conference of the IEEE Engineering in Medicine and Biology Society.

Krishnamoorthy V, Latash ML, Scholz JP, Zatsiorsky VM, 2003. Muscle synergies during shifts of the center of pressure by standing persons. Exp. Brain Res 152, 281–292. [PubMed: 12904934]

Kronberg M, Németh G, Broström L, 1990. Muscle activity and coordination in the normal shoulder. An electromyographic study. Clin. Orthop. Relat. Res, 76–85.

Kuechle DK, Newman SR, Itoi E, Morrey BF, An K-N, 1997. Shoulder muscle moment arms during horizontal flexion and elevation. J. Shoulder Elbow Surg 6, 429–439. [PubMed: 9356931]

Leonardis JM, Alkayyali AA, Lipps DB, 2020. Posture-dependent neuromuscular contributions to three-dimensional isometric shoulder torque generation. 123, 1526–1535.

Leonardis JM, Lyons DA, Giladi AM, Momoh AO, Lipps DB, 2019. Functional integrity of the shoulder joint and pectoralis major following subpectoral implant breast reconstruction. J. Orthop. Res 37: 1610–1619. [PubMed: 30816589]

McGuire KP, Santillan AA, Kaur P, Meade T, Parbhoo J, Mathias M, Shamehdi C, Davis M, Ramos D, Cox CE, 2009. Are mastectomies on the rise? A 13-year trend analysis of the selection of mastectomy versus breast conservation therapy in 5865 patients. Ann. Surg. Oncol 16, 2682–2690. [PubMed: 19653046]

Metcalfe KA, Lubinski J, Ghadirian P, Lynch H, Kim-Sing C, Friedman E, Foulkes WD, Domchek S, Ainsworth P, Isaacs CJ, 2008. Predictors of contralateral prophylactic mastectomy in women with a BRCA1 or BRCA2 mutation: the Hereditary Breast Cancer Clinical Study Group. J Clin Onc 26, 1093–1097.

Olivari N, 1976. The latissimus flap. British journal of plastic surgery 29, 126–128. [PubMed: 776304]

Quillen CG, 1979. Latissimus dorsi myocutaneous flaps in head and neck reconstruction. Plastic and reconstructive surgery 63, 664–670. [PubMed: 372993]

Roh J, Rymer WZ, Beer RF, 2012. Robustness of muscle synergies underlying three-dimensional force generation at the hand in healthy humans. J. Neurophysiol 107, 2123–2142. [PubMed: 22279190]

Roh J, Rymer WZ, Perreault EJ, Yoo SB, Beer RF, 2013. Alterations in upper limb muscle synergy structure in chronic stroke survivors. J. Neurophysiol 109, 768–781. [PubMed: 23155178]

Schwartz MH, Rozumalski A, Steele KM, 2016. Dynamic motor control is associated with treatment outcomes for children with cerebral palsy. Dev. Med. Child Neurol 58, 1139–1145. [PubMed: 27097830]

Shamley DR, Srinanaganathan R, Weatherall R, Oskrochi R, Watson M, Ostlere S, Sugden E, 2007. Changes in shoulder muscle size and activity following treatment for breast cancer. Breast cancer research and treatment 106, 19–27. [PubMed: 17221154]

Spear SL, Hess CL, 2005. A review of the biomechanical and functional changes in the shoulder following transfer of the latissimus dorsi muscles. Plast. Reconstr. Surg 115, 2070–2073. [PubMed: 15923857]

Steele KM, Rozumalski A, Schwartz MH, 2015. Muscle synergies and complexity of neuromuscular control during gait in cerebral palsy. Dev. Med. Child Neurol 57, 1176–1182. [PubMed: 26084733]

Steele KM, Tresch MC, Perreault EJ, 2013. The number and choice of muscles impact the results of muscle synergy analyses. Front. Comput. Neurosci 7, 105. [PubMed: 23964232]

Stegink-Jansen CW, Buford WL Jr, Patterson RM, Gould LJ, 2011. Computer simulation of pectoralis major muscle strain to guide exercise protocols for patients after breast cancer surgery. J. Orthop. Sports Phys. Ther 41, 417–426. [PubMed: 21628825]

Surgeons A.S.o.P., American Society of Plastic Surgeons, 2018 Plastic Surgery Statistics Report, (2019)

Tresch MC, Saltiel P, d'Avella A, Bizzi E, 2002. Coordination and localization in spinal motor systems. Brain Res. Rev 40, 66–79. [PubMed: 12589907]

Wickham J, Pizzari T, Stansfeld K, Burnside A, Watson L, 2010. Quantifying 'normal'shoulder muscle activity during abduction. J. Electromyogr. Kinesiol 20, 212–222. [PubMed: 19625195]

Xu X, McGorry RW, Lin J-H, 2014. A regression model predicting isometric shoulder muscle activities from arm postures and shoulder joint moments. J. Electromyogr. Kinesiol 24, 419–429. [PubMed: 24618104]

Yao K, Stewart AK, Winchester DJ, Winchester DP, 2010. Trends in contralateral prophylactic mastectomy for unilateral cancer: a report from the National Cancer Data Base, 1998–2007. Ann. Surg. Onc 17, 2554–2562.

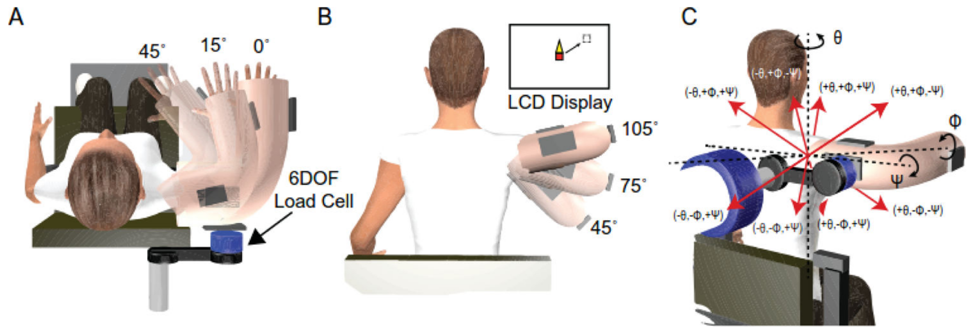

Figure 1.

Schematic of the experimental setup, arm postures, and 3D isometric shoulder torques. Each participant's dominant and non-dominant shoulders were assessed in five arm postures that were a combination of plane (A) and elevation (B) positions. In each posture, participants generated 3D shoulder torques in every combination of ± plane of elevation (Θ), ± elevation (Φ), and ± rotation (ϒ) (C). Visual feedback was provided via an LCD monitor to assist with torque accuracy. This feedback was presented as a blank, white screen overlaid by a red square cursor that was controlled by the shoulder torques produced by participants. A dashed box represented the prescribed magnitude and direction of each 3-D torque task. Elevation torques translated the cursor in the up and down directions, plane of elevation torques translated the cursor to the left and right, and axial rotation torques resulted in the growth of a triangle off the top or bottom of the cursor.

Author Manuscript
Author Manuscript
Author Manuscript

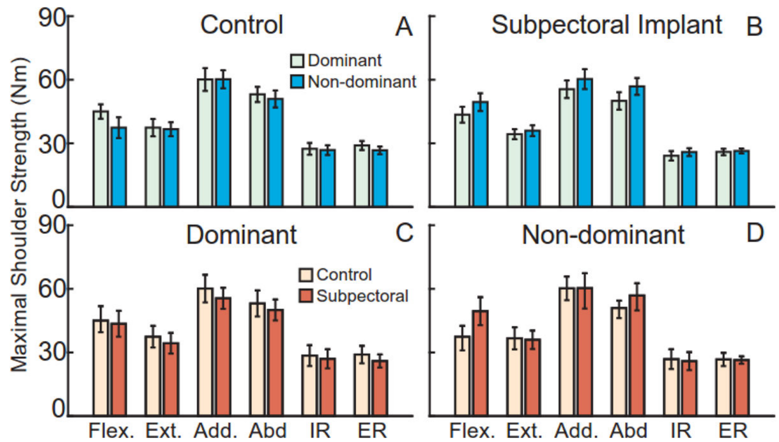

Figure 2.

Participants generated maximal shoulder torques in shoulder flexion, extension, adduction, abduction, internal rotation, and external rotation on their dominant and non-dominant arms. Within each group, arm dominance did not influence shoulder strength (A, B). Strength did not differ between the groups on the dominant (C) or non-dominant (D) arms. Bars represent mean ± standard error.

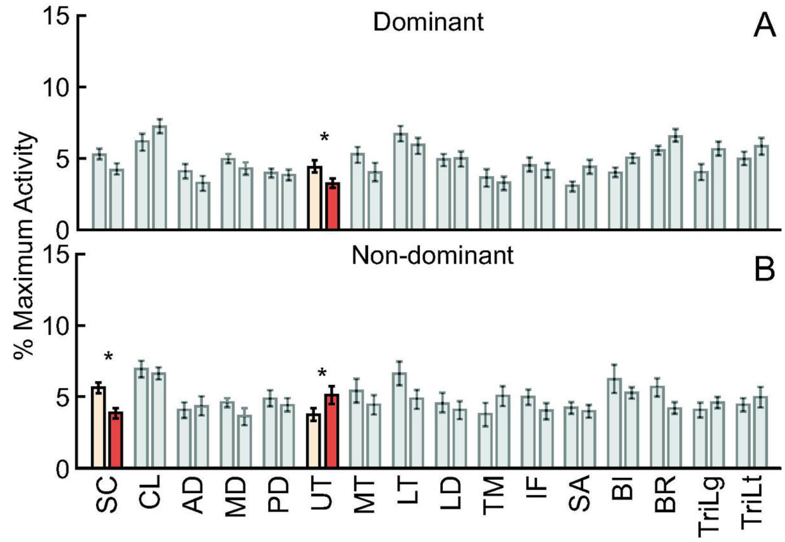

Figure 3.

Surface electromyography data were obtained from sixteen shoulder muscles while participants generated eight 3D isometric shoulder torques in five two-dimensional arm postures bilaterally. On the dominant arm, only upper trapezius activity differed between the groups (A). On the non-dominant arm, the sternocostal fiber region of the PM and upper trapezius activity differed between the groups (B). Bars represent mean ± standard error. Significant differences are visualized by colored bars and * signifies a significant group difference at $p < 0.05$.

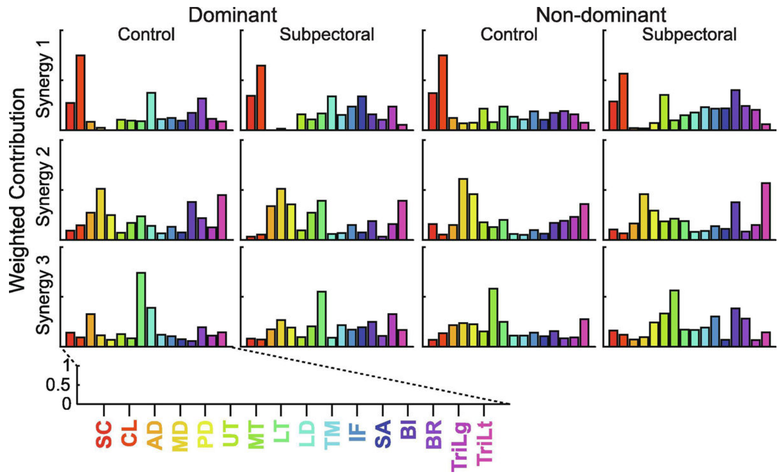

Figure 4.

Matrix of shoulder muscle synergies derived from representative participants in each of the experimental groups on the dominant and non-dominant arms. Each row represents a separate synergy, while the columns divide participants by the experimental group and arm. The weighted contributions of each muscle to each synergy are represented on a scale from 0 to 1. SC: sternocostal fiber region of the pectoralis major, CL: clavicular fiber region of the pectoralis major, AD: anterior deltoid, MD: medial deltoid, PD: posterior deltoid, UT: upper trapezius, MT: middle trapezius, LT: lower trapezius, LD: latissimus dorsi, TM: teres major, IF: infraspinatus, SA: serratus anterior, BI: biceps brachii long head, BR: brachioradialis, TriLg: triceps brachii long head, TriLt: triceps brachii lateral head.

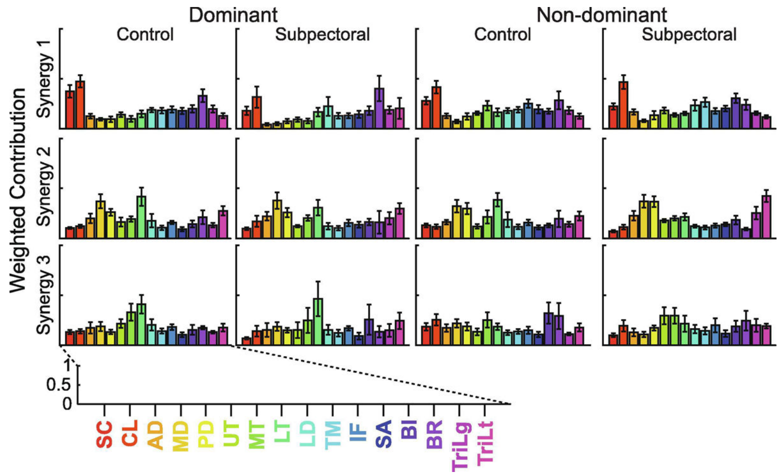

Figure 5.

Group ± standard error shoulder muscle synergies in each of the experimental groups on the dominant and non-dominant arms. Each row represents a separate synergy, while the columns divide participants by the experimental group and arm. The weighted contributions of each muscle to each synergy are represented on a scale from 0 to 1. SC: sternocostal fiber region of the pectoralis major, CL: clavicular fiber region of the pectoralis major, AD: anterior deltoid, MD: medial deltoid, PD: posterior deltoid, UT: upper trapezius, MT: middle trapezius, LT: lower trapezius, LD: latissimus dorsi, TM: teres major, IF: infraspinatus, SA: serratus anterior, BI: biceps brachii long head, BR: brachioradialis, TriLg: triceps brachii long head, TriLt: triceps brachii lateral head.

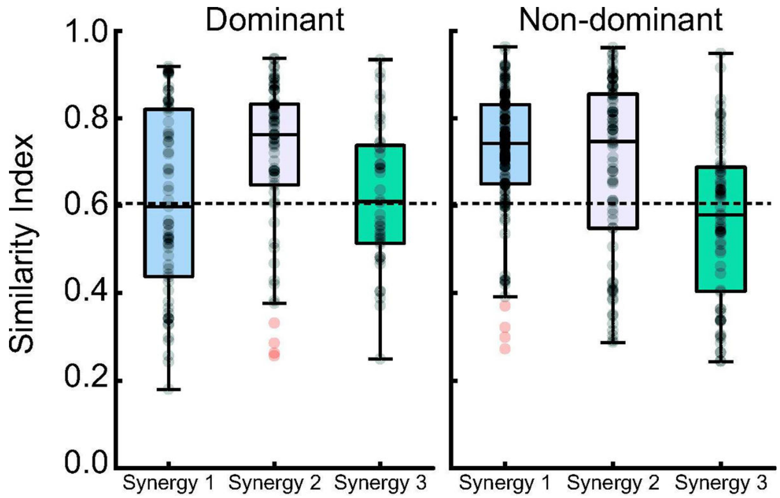

Figure 6.

Boxplots of the median +/− interquartile range similarity index between our experimental groups, separated by arm dominance. Horizontal dashed lines represent the SI > 0.63 cutoff, which was used to determine if two synergies were more similar than is expected by chance. Individual data are represented as transparent black dots, while outliers are represented as transparent red dots.

Table 1.

Mean (standard error of the mean) participant demographics for the included experimental groups: healthy controls (Control) and two-stage subpectoral implant (Subpectoral).

	Control	Subpectoral	*t*	*p*
Number of Participants	10	14		
Age (yrs)	55 (2)	49 (3)	1.61	0.12
Height (m)	1.62 (0.02)	1.66 (0.01)	−1.88	0.09
Weight (kg)	62 (2)	73 (4)	−2.11	0.03
BMI (kg/m^2)	24 (0.6)	27 (1.5)	−1.56	0.09
Days Post-Treatment	-	1019 (83)		
Radiation Therapy	-	2		
Chemotherapy	-	4		
Axillary Lymph Node Dissection (ALND)	-	3		
Sentinel Lymph Node Biopsy (SLNB)	-	7		